A neurofunctional signature of affective arousal generalizes across valence domains and distinguishes subjective experience from autonomic reactivity

Authors

Ran Zhang[1,2], Xianyang Gan[3,4], Ting Xu[1,2], Fangwen Yu[3,4], Lan Wang[3,4], Xinwei Song[3,4], Guojuan Jiao[3,4], Xiqin Liu[5], Feng Zhou[1,2]*, Benjamin Becker[6,7]*

Affiliations

[1]Faculty of Psychology, Southwest University, Chongqing, China

[2]Key Laboratory of Cognition and Personality, Ministry of Education, Chongqing, China

[3]The Center of Psychosomatic Medicine, Sichuan Provincial Center for Mental Health, Sichuan Provincial People's Hospital, University of Electronic Science and Technology of China, Chengdu, China

[4]School of Life Science and Technology, University of Electronic Science and Technology of China, Chengdu, China

[5]Huaxi MR Research Center (HMRRC), Department of Radiology, West China Hospital of Sichuan University, Chengdu, China.

[6]State Key Laboratory of Brain and Cognitive Sciences, The University of Hong Kong, Hong Kong, China

[7]Department of Psychology, The University of Hong Kong, Hong Kong, China

***Correspondence to**

Feng Zhou
Southwest University
Tian Sheng RD, No.2, Beibei, ChongQing, 400715, China
Mail: zhou.feng@live.com

Benjamin Becker
The University of Hong Kong
Pokfulam, Hong Kong, China
Mail: bbecker@hku.hk

Abstract

Arousal is fundamental for affective experience and, together with valence, defines the core affective space. However, a precise brain model of affective arousal is lacking, leading to continuing debates of whether the neural systems generalize across valence domains and are separable from those underlying autonomic arousal. Here, we combined naturalistic fMRI with predictive modeling to develop a brain affective arousal signature (BAAS, discovery-validation design, n = 96) and demonstrate its (1) sensitivity and generalizability across mental processes and valence domains, and (2) neural distinction from autonomic arousal (18 studies, n = 735). Affective arousal was encoded in distributed cortical (e.g., prefrontal regions, insula) and subcortical (e.g., amygdala, periaqueductal gray) systems. Given that high arousal progressively overshadows specific emotions we applied the BAAS to improve specificity of established neuroaffective signatures. Our study provides a biologically plausible affective arousal model that aligns with the affective space and has a high application potential.

Keywords

Affective arousal, Valence, Autonomic arousal, Signature, Multivariate pattern analysis, Naturalistic paradigm

Main Text

Introduction

The stream of subjective affective experiences (feelings) represents a continuous assessment of the internal state and its relation with the environment, facilitating adaptive responses, avoiding harm, and identifying opportunities[1]. The mental topology of the highly subjective affective experiences remains controversially debated[2], but most current theories converge on a dimensional space with core affective domains representing pleasure-displeasure (i.e., valence) and activation-deactivation (i.e., arousal or intensity)[3,4], which together underlie conscious affective experiences[5,6]. These 'core affect' dimensions[5] represent critical defining features that distinguish affective experiences from other mental states[7] and form a two-dimensional affective space encompassing specific emotional states (e.g. anger: negative valance and high arousal). Within this core affective space arousal and valance exhibit a V-shaped architecture such that arousal increases in conjunction with either positive or negative valence[8,9] (see Fig. 1), while increasing levels of intense arousal may progressively overshadow specific emotional states on the subjective, perceptual, and neural level[10,11].

The behavioral and neural dynamics of the valance dimension have been extensively mapped at different granularity levels ranging from neural signatures for general negative affect[12] to signatures that distinguish emotion-specific mental states[13,14] or subjective affective experiences from accompanying physiological responses[15,16], respectively. In contrast, and despite its central position in both, classical theoretical accounts and everyday subjective experience of emotion[17,18] an integrative and generalizable neural model for conscious affective arousal in humans is lacking. The few conceptualizations and studies to date primarily focus on physiological (autonomic) or wakefulness (vigilance) aspects[19] of arousal rather than the conscious affective experience.

Sophisticated animal studies have established comprehensive and intricate neurobiological models for wakefulness and autonomic arousal, encompassing subcortical systems such as the brainstem, thalamic, and hypothalamic nuclei[20-22]. While there is some overlap between the brain systems controlling wakefulness and hard-wired autonomic reactivity with those involved in affective arousal[21,23,24], accumulating evidence suggests that the subjective experience that characterizes affective arousal in humans may operate through distinct neural mechanisms[19,25]. In contrast to the anatomical precision of the animal models, human studies on the subjective affective components of arousal have focused on large-scale brain systems (for review see e.g., Satpute et al.[19]), including default mode network subsystems (i.e. anterior medial prefrontal cortex) and the 'salience network' (including the anterior cingulate cortex, insula, and amygdala)[26,27], as well as brainstem regions[28].

Traditionally, neuroimaging research on affective processes in humans has relied on experimental paradigms employing isolated and sparsely presented stimuli in a single modality (e.g., affective pictures) and analytic approaches that aim at localizing brain regions that show the highest increase in activity by conducting numerous tests across individual 'voxels' or regions – strategies characterized by a low ecological validity for dynamic emotional processes in everyday life[29] and low to moderate effect sizes[30] and reliability[31] in terms of characterizing affective mental processes[12,14,16,32]. Recent advances have successfully leveraged neuroimaging combined with machine learning algorithms (i.e., multivariate pattern analysis, MVPA) to develop predictive and

more precise and comprehensive neural signatures for subjective affective experiences characterized by a specific emotional state and high negative affective arousal, including general negative affect[12,32], pain[33], disgust[13] , fear[14,15] and anxious anticipation[16]. The advances allowed to predict the specific subjective affective state with greater effect sizes and robustness compared to traditional local region-based approaches[34,35] and to demonstrate that the specific emotional states are characterized by common and distinct brain-wide neural representations between subjective emotional states or high affective arousal, respectively[15,16]. This holds the potential to improve the description of mental processes at the brain level[36]. This approach has refined our understanding of affective experiences by demonstrating that they are encoded in distributed brain systems, which is aligned with meta-analytic evidence indicating that affective experiences are linked to activations across a wide array of brain regions[37].

However, it remains to be determined whether affective arousal - a core aspect of affective experiences - exhibits distributed neural representations in the human brain and whether these representations are independent of valance and distinguishable from the neural representations of the accompanying physiological arousal. Moreover, consistent with conceptualizations of the affective space proposing that both positive and negative affect are associated with high levels of arousal, our recent study showed that neural signatures for negative emotions exhibited strong activations in response to positive stimuli compared to neutral ones[38]. This suggests that these signatures may partly capture the arousal inherent to strong affective experiences[39-41]. Together with the observed overshadowing effect of high arousal on the specific emotions across domains[10,11] this lead to conceptual debates of whether the arousal dimension is represented across valence in the brain and whether accounting for arousal may increase the specificity of decoding specific emotional states from the brain.

Against this background we here aimed to (1) develop a sensitive and generalizable brain signature (i.e., BAAS) that can precisely capture the subjective experience of affective arousal under ecologically valid conditions combining naturalistic fMRI with an MVPA-based neural decoding approach, (2) determine whether the neural representations of affective arousal vary as a function of valence or whether positive and negative arousal are mediated by the same brain mechanism, (3) to establish a comprehensive and biologically informed model on how affective arousal is represented in human brain. Given the intricate interaction between autonomic and affective arousal and initial studies demonstrating that the neural representations of autonomic and affective experience might be distinguishable[15,16] we further examined (4) whether the subjective affective arousal experience is separable from autonomic arousal in humans. Finally, based on previous literature suggesting that high levels of progressively increasing arousal overshadow the representation of specific emotions[11], we tested if (5) accounting for a precise neural signature of increasing arousal can enhance the specificity of existing affective neural signatures.

To this end we combined naturalistic fMRI with machine learning-based neural decoding to identify a brain signature predictive of affective arousal intensity in healthy participants (study 1, n = 60) as they experienced a range of positive and negative emotions induced by carefully selected video clips. To enhance the ecological validity of the signature and facilitate immersive and intense arousal experience we utilized naturalistic fMRI experiments using visual-auditory movie clips and requested subjects to report their affective arousal experiences (Fig. 1a). The predictive performance and generalizability of the identified neural signature were assessed in an independent validation

cohort (study 2, n = 36), using a modified arousal induction paradigm, with new and longer movie clips covering different aspects of the emotional space. We next tested the signature across 15 studies (total n = 609, details see Table S1) involving various stimulus modalities to identify its generalization, sensitivity and specificity across high arousing affective states, paradigms, populations and image acquisition systems (Fig. 1b). The neural representations underlying affective arousal were systematically determined using backward (prediction) and forward (association) encoding models. The neurobiological validity of the BAAS was further examined against meta-analytic maps of negative and positive emotions from large-scale meta-analysis[42] and the separability from autonomic arousal was determined using a validated decoder for autonomic arousal (fMRI data from Taschereau-Dumouchel, V et al.[15], n = 25) (Fig. 1c). Moreover, we investigated whether adjusting for arousal ratings and BAAS responses could enhance the precision of two previously developed and widely employed affective signatures for specific emotional states[13,32] (Fig. 1d). Overall, this study aims to establish a comprehensive neural model of affective arousal, enhancing our comprehension of how the brain represents affective arousal and refining the prediction specificity of neural signatures for affective experiences.

Results

Behavioral results

In study 1, a total of 40 immersive video stimuli (~25 s) were employed to induce varying levels of arousal experience. Participants were asked to experience video stimuli immersively and report their current level of affective arousal for each stimulus on a 9-point Likert scale ranging from 1 (very low arousal) to 9 (very high arousal). As shown in Fig. S1a, stimuli induced a wide range of subjective arousal in the discovery cohort which was used to develop the neural signature of subjective affective arousal. Study 2, the validation cohort, employed 28 novel ~60 s video stimuli to elicit different levels of subjective affective arousal feelings in an independent sample (Fig. S1b).

Identifying a brain signature for affective arousal

In line with previous studies[12-15], we employed support vector regression (SVR) in study 1 to develop a brain activity-based signature for subjective affective arousal that predicted the intensity of self-reported arousal experience during the videos. To evaluate the performance of the brain affective arousal signature (BAAS), we conducted the 10 × 10-fold cross-validation procedure in the discovery cohort and additionally validated the signature in the independent study.

The developed BAAS was sensitive to subjective arousal experience in both discovery and independent validation cohorts, as evidenced by significant associations between observed and predicted ratings (Fig. 2a, b). Specifically, in the discovery cohort, the averaged within-subject correlation was 0.88 ± 0.01 (standard error (SE)), the average root mean squared error (RMSE) was 1.36 ± 0.05, the coefficient of determination (R^2) was [0.61 0.64], the overall (between- and within-subjects) prediction-outcome correlation was 0.82 (R^2 = 0.65) (Fig. 2a). These findings were replicated in the validation cohort such that BAAS effectively predicted subjective arousal ratings yielding a high prediction-outcome correlation (average within-subject correlation coefficient r = 0.80 ± 0.03 SE, RMSE = 1.68 ± 0.08 SE, R^2 = 0.42; overall prediction-outcome correlation coefficient r = 0.70, R^2 = 0.49, Fig. 2b), indicating a sensitive and robust neurofunctional arousal signature. In addition, we categorized video clips in the validation cohort into low (ratings 1, 2, and

3), medium (ratings 4, 5, and 6), and high (ratings 7, 8, and 9) arousal conditions, according to self-reported arousal ratings and applied the two-alternative forced-choice test to examine whether the BAAS could distinguish different arousal conditions. We found that the BAAS response accurately classified high versus moderate (81 ± 6.9%, $p = 5.35 \times 10^{-4}$, d = 1.29), moderate versus low (92 ± 4.6%, $p = 3 \times 10^{-6}$, d = 2.56), and high versus low (100 ± 0.0%, $p < 1\times10^{-6}$, d = 3.21) conditions. Of note, in this analysis, we excluded 4 subjects because they did not have ratings of high or moderate arousal.

We next tested whether valence, another core dimension of affective experience, contributes to BAAS predictions and whether arousal cuts across the valence dimension of the affective space. Given that both positive and negative video clips induced high arousal (positive: mean ± SD = 7.37 ± 0.35; negative: mean ± SD = 7.94 ± 0.29, details of videos in validation cohort see Table S2), we hypothesized that if BAAS primarily captures arousal rather than valence information, it should accurately classify high arousing positive and negative video clips from low arousing neutral video clips, yet it might not differentiate between the negative and positive video clips. Consistent with our hypotheses, BAAS demonstrated significant discriminability of unspecific high arousal experiences (positive versus neutral: 97 ± 2.7%, $p < 1\times10^{-6}$, d = 2.63; negative versus neutral: 97 ± 2.7%, $p < 1\times10^{-6}$, d = 2.90) and poor accuracy in discriminating between two high-arousal experiences (negative versus positive: 53 ± 8.3%, p = 0.8679, d = 0.04), suggesting high specificity of the BAAS for capturing arousal across valence.

Given that previous studies showed activity in the visual cortex in response to arousing emotional scenes, suggesting that visual processing contributes to arousal[43-46], we tested to which extent the BAAS depended on the visual cortex. Therefore, we retrained the decoder excluding the entire occipital lobe. We observed similar performance including significant prediction-outcome correlations and coefficient of determination in this modified setup, suggesting that the prediction is not solely reliant on emotional schemas encoding within visual regions (further details see Supplementary Results and Fig. S2).

Within-subject trial-wise prediction

Affective arousal experience is a highly subjective state and can rapidly fluctuate within a short period, typically on the order of minutes or even seconds[25,47,48]. We next examined to what extent the population-level BAAS can accurately predict individual-level variations in arousal, specifically on a trial-by-trial basis. To this end, single-trial analysis was used to obtain individual-specific trial-wise activation maps. Subsequently, the BAAS pattern expressions of these single-trial activation maps were calculated and then correlated with corresponding true ratings for each subject separately. In the discovery cohort, the BAAS accurately predicted individual arousal experience (n = 40 trials; within-participant r = 0.55 ± 0.01 SE, 10 × 10 cross-validated; Fig. 2c). Of note, the BAAS successfully predicts trial-by-trial arousal ratings in all participants within the discovery cohort (all $p \leq 3.8\times10^{-3}$). The predictive performance of the BAAS on the validation cohort was similar to those observed in the discovery cohort (within-participant r = 0.58 ± 0.03 SE, Fig. 2c), and the BAAS significantly predicted over 83.3% of participants in the validation dataset. Taken together, our findings suggest that BAAS accurately predicts the level of momentary arousal feelings on the individual level.

Generalization of BAAS performance

We examined whether the BAAS could capture affective arousal across various stimulus modalities and different experimental approaches. A substantial body of evidence suggests a V-shaped relationship between affective valence and arousal levels, wherein individuals experiencing more intense positive or negative emotions generally report heightened arousal[9] (Fig. 1). We therefore determined whether the BAAS distinguishes high arousal negative experiences from low arousal negative experiences across affective domains, stimulus modalities and generalizes to the stimulus-free state (aversive anticipation) (Fig. 2d 'Studies 3-6'). Study 3 employed a naturalistic affective video-watching fMRI paradigm involving strong disgust-inducing, arousal-matched negative, and neutral video stimuli (affective ratings see Table S2). We found that the BAAS successfully classified disgust and negative from neutral experiences with high accuracies (disgust versus neutral: accuracy = 97 ± 1.8% SE, $p < 1 \times 10^{-6}$, d = 2.64, negative versus neutral: accuracy = 100 ± 0.0% SE, $p < 1 \times 10^{-6}$, d = 3.08) supporting its generalizability. Of note, the BAAS could not classify arousal matched negative (arousal: mean ± SD = 7.15 ± 0.41) from disgust experience-specific neural activity in this dataset (arousal: mean ± SD = 7.23 ± 0.50) (accuracy = 60 ± 5.5% SE, p = 0.0888, d = 0.31, Fig. S3), further supporting that the signature captures arousal across negative affective states. Study 4 induced negative experience with four types of aversive stimuli—painful heat, painful pressure, aversive images and aversive sounds[32]. The BAAS was able to effectively distinguish between high and low levels (i.e., level 4 and level 1) of aversive image (accuracy = 78 ± 5.6% SE, $p = 3.3 \times 10^{-5}$, d = 1.08), thermal pain (accuracy = 76 ± 5.7% SE, $p = 1.11 \times 10^{-4}$, d = 0.96), mechanical pain (accuracy = 73 ± 6.0% SE, p = 0.0010, d = 0.90), and aversive sound (accuracy = 67 ± 6.3% SE, p = 0.0145, d = 0.48). Additionally, the BAAS could accurately predict the aversive ratings induced by aversive image ($r = 0.30$, $p = 6.7 \times 10^{-6}$), thermal pain ($r = 0.24$, $p = 4.1 \times 10^{-4}$), mechanical pain ($r = 0.40$, $p < 1 \times 10^{-6}$), and aversive sound ($r = 0.16$, p = 0.0163). These results indicated that the BASS generalizes to pain-associated states and across stimulus modalities. In line with the extension to pain – in study 5[49] - the BAAS successfully predicted subjective pain ratings (prediction-outcome $r = 0.41$, $p < 1 \times 10^{-6}$) as well as accurately discriminated high levels of pain versus low levels of pain (44.8°C vs. 48.8°C) (accuracy = 85 ± 6.2% SE, $p = 6.6 \times 10^{-5}$, d = 1.16). Moreover, we further tested whether the BAAS is independent of the actual stimulus exposure by testing generalization to data from an 'Uncertainty-Variation Threat Anticipation' (UVTA) task in study 6 [16]. During this task participants anticipate aversive electrical stimulation with varying levels of uncertainty and retrospectively rated their anxious arousal during the anticipation period. The BAAS accurately predicted the subjective anxious experience with prediction-outcome $r = 0.45$ ($p < 1 \times 10^{-6}$), confirming its generalization to stimulus-free internal mental processes. Together, these findings demonstrate the generalizability of BAAS across negative experiences, stimuli and modalities.

We next determined generalizability of the BAAS in the positive domain by capitalizing on data from 10 independent studies, employing different strategies and modalities to induce high arousing positive affect across the experience and anticipation period (e.g., music, images of appetizing food, erotic images, cues of monetary rewards, and socially relevant stimuli with 2 studies in each category)[50-59]. The results indicated that BAAS exhibited significantly stronger responses to positive compared to control conditions in nine out of ten studies (refer to Table 1 and Fig. 2d 'Studies 7-16'), and a marginally significant stronger response (p = 0.068) in the remaining study, suggesting that the BAAS can capture high-arousal positive experiences across stimulus modalities (i.e., vision and auditory).

These findings were further replicated in a large dataset with arousal-matched negative and positive affect induction[60] (n = 150, Fig. 2d 'Study 17'), where the BAAS accurately classified negative and positive from neutral conditions (negative vs. neutral: accuracy = 83 ± 3.1% SE, $p < 1 \times 10^{-6}$, d = 1.12; positive vs. neutral: accuracy = 92 ± 2.2% SE, $p < 1 \times 10^{-6}$, d = 1.78). Overall, BAAS showed remarkable generalizability across valence domains and multiple modalities.

Of note, these datasets were collected with diverse MRI scanners, populations and were preprocessed using various pipelines. Our findings collectively highlight the robust generalizability and high sensitivity of the BAAS originally developed in the movie-watching paradigm in effectively predicting high affective arousal experiences across diverse stimuli, modalities, valence, MRI systems, preprocessing pipelines, and populations.

The neurofunctional characterization of the affective arousal signature

To understand the neurofunctional core system of affective arousal in humans we carefully determined the brain regions reliably contributing to the BAAS prediction performance. To this end, we conducted bootstrap tests to identify voxels that most reliably contribute to the prediction ($q < 0.05$, false discovery rate (FDR) corrected). As shown in Fig. 3a, activity in amygdala, periaqueductal gray (PAG), parahippocampal gyrus, lateral orbitofrontal cortex (lOFC), dorsomedial prefrontal cortex (dmPFC), subgenual anterior cingulate (sACC), and superior frontal gyrus (SFG) strongly predict increased affective arousal. Conversely, most reliable negative weights (i.e., higher arousal with decrease activity) were found in the posterior insula / rolandic operculum, supplementary motor area (SMA), middle frontal gyrus (MFG), inferior parietal lobule (IPL) and posterior cingulate cortex (PCC). These regions have been reported in the literature for a range of high arousing emotional experiences.

In addition to the population-level BAAS model, we developed a predictive model for each participant based on single-trial data and performed a one-sample t-test analysis (treating participants as a random effect) on weights derived from individualized multivariate predictive models ($q < 0.05$, FDR corrected). This approach enables us to identify arousal-predictive regions consistently across participants. In line with the BAAS model, we observed that amygdala, parahippocampal gyrus, PAG, anterior insula, dmPFC, and SFG robustly predict enhanced affective arousal, while reductions in affective arousal were strongly linked to signals from posterior insula, SMA, MFG, PCC (Fig. 3b). Brain regions associated with affective arousal determined with univariate parametric modulation approach identified a similar set of broadly distributed regions (see Supplementary Results and Fig. S4).

To further validate the identified biologically plausible affective arousal brain system, we firstly compared the thresholded BAAS ($q < 0.05$, FDR corrected) with the conjunction of the meta-analytic maps of 'negative' and 'positive' affective experiences which were obtained from the Neurosynth (association test $q < 0.05$, FDR corrected, maps see Fig. S5b). Given that feeling of arousal are more likely to be accompanied by valanced feelings, positive or negative[9], we hypothesized that the overlapping between these two meta-analytic maps might share common brain regions with the BAAS. Consistent with our prediction, several overlapping regions (e.g., amygdala, parahippocampal gyrus, including inferior frontal gyrus (IFG), lOFC, and sACC) between two patterns were observed using conjunction analyses (Fig. 4a). As shown in Fig. S5, brain regions including IFG, SFG, dmPFC, amygdala, parahippocampal gyrus, and insula positively associated

with both 'negative' and 'positive' meta-analytic maps were also found significant in the BAAS, though there were not directly overlapping. Conversely, SMA and precentral gyrus regions were negatively associated with both 'negative' and 'positive' meta-analytic maps and were reliably predictive of decreased arousal in the BAAS. These findings offer evidence confirming the identified regions involved in affective arousal processing.

Together, our results identify the conscious experience of affective arousal is represented in distributed subcortical and cortical regions involved in salience information processing (e.g., amygdala, insula)[61,62], emotional awareness (e.g., frontal regions)[63], and emotional memory (e.g., hippocampus)[64], as well as areas that have been emphasized as a core system mediating the arousal function in animal models (brainstem)[19].

Alternative models to determine the contribution of isolated arousal-prediction models: BAAS predicts more precise that isolated networks

Previous studies have emphasized contributions of DMN, salience and subcortical network to affective arousal processing[26,27] and psychological construction theories of emotion proposed arousal as one component of 'core affect' underlying functions that are neurobiologically supported by large-scale networks[37]. To address this question, we retrained the predictive SVR model by restricting its activations to (1) a subcortical network, and (2) each of seven large-scale resting-state functional networks (see Methods session) in discovery cohort. This allowed us to examine the extent to which these models could predict arousal experiences compared to the whole-brain BAAS. The results showed that brain networks, especially the subcortical network and dorsal attention network, to some extent, predict subjective affective arousal ratings (see Fig. 4b and Table S3). Considering the potential effects of the number of features/voxels in prediction analyses, as shown in Fig. 4b, we implemented a control procedure. Specifically, we conducted 1000 repeated random voxel selections from different brain regions, including the entire brain, subcortical, or individual resting-state networks (averaged over 1000 iterations). This approach was carried out to assess the impact of varying the sampled brain systems. Interestingly, our results revealed that the asymptotic prediction achieved when sampling from all brain systems, as demonstrated in the BAAS (black line in Fig. 4b), was substantially higher than the asymptotic prediction within individual networks (colored line in Fig. 4b). This analysis provided that whole-brain models exhibit significantly larger effect sizes than models using features from a single network. Moreover, consistent with previous studies on affective neural signatures[13,14], the optimum BAAS performance was achieved when approximately 10,000 voxels were randomly sampled across the whole brain. Crucially, the performance was contingent upon a diverse selection of voxels derived from multiple brain systems. These findings further support the notion that information about affective arousal experiences is combined in the neural signature that extends across multiple systems.

In addition, we calculated the overlapping ratio between significant features of the BAAS and each large-scale functional network, as well as the subcortical network (Fig. 4c). The positive predictive weights of the model showed important overlaps with voxels of the visual (34.36%), default (13.97%), ventral attention (15.08%), dorsal attention (13.69%) and subcortical networks (12.57%), and the negative one had a remarkable overlap with somatomotor (31.61%) and frontoparietal network (22.58%). These findings further support the notion that arousal is represented across widely distributed brain networks.

Affective arousal and autonomic arousal engage distinct neural representations in humans

Previous conceptualizations have hypothesized that affective arousal and autonomic arousal may operate through distinct neural mechanisms[19]. Given skin conductance level (SCL) serves as a stable and valid index of autonomic arousal[65], we developed a novel whole-brain pattern to decode autonomic arousal using brain activation maps corresponding to various levels of SCL in study 18 (n = 25, 5×5-fold cross-validated, see Supplementary Methods). The developed autonomic arousal signature accurately predicted the level of autonomic arousal (averaged within subject r = 0.77 ± 0.03, mean RMSE = 1.58 ± 0.11; overall prediction-outcome = 0.56, Fig. S6). To further validate the developed decoder, a two-alternative forced-choice test was applied in study 19. In this study, participants underwent a Pavlovian threat conditioning task with simultaneously acquired fMRI and psychophysiological arousal responses (skin conductance response, SCR). Of note, consistent with our previous study[66] in this analysis we only included participants (n = 58) who exhibited stronger psychophysiological threat responses (i.e., mean CS+ > mean CS-, conditioned stimulus, CS) during threat acquisition. The autonomic arousal decoder response accurately classified CS+ (associated with high SCL) versus CS- (associated with low SCL) with 76 ± 5.6% accuracy ($p = 1 \times 10^{-4}$, d = 0.95) (Fig. 5a). Of note, we found that the BAAS could not classify high versus low psychophysiological arousal response very well in study 19 (60 ± 6.4% SE, p = 1.1480, d = 0.49, see Fig. S7).

Next, we investigated whether neural representations of affective arousal and autonomic arousal can be dissociated. We applied the BAAS and autonomic arousal signature to an independent fMRI dataset collected during a UVTA task from study 20[16]. This produced beta maps corresponding to anxious arousal ratings and categorized brain activation maps based on five different levels of SCL during the anticipation period for each subject (see Supplementary Methods for details). We hypothesized that if affective arousal and autonomic arousal share similar mechanisms, the BAAS and autonomic arousal signature should perform well in distinguishing arousal experiences. Specifically, the BAAS response should discriminate high SCL (ratings 4 and 5) from low SCL (ratings 1 and 2), and the autonomic arousal signature should predict high anxious experience (ratings 4 and 5) from low anxious experience (ratings 1 and 2). Conversely, limited predictive performance would indicate independence of the neural representations for affective arousal and autonomic arousal constructs. Of note, given the autonomic arousal decoder was developed based on levels of skin conductance reactivity, we focused on the classification performance of two decoders here. As shown in Fig. 5b, the BAAS predicted high anxious experience versus low anxious experience with high accuracy (77 ± 6.4%, $p = 6.06 \times 10^{-4}$, d = 0.99), but did not classify high SCL from low SCL above chance level (60 ± 7.5%, p = 0.2221, d = 0.05). Conversely, the autonomic arousal signature successfully predicted high SCL versus low SCL with 67 ± 7.1% accuracy (p = 0.0315, d = 0.61), but could not discriminate high anxious experience (53 ± 7.6% accuracy, p = 0.7608, d = 0.26).

To further support the hypothesis of separable neural representations underlying affective arousal and autonomic arousal, we explored the joint distribution of normalized (z-scored) voxel weights of these two patterns by plotting BAAS on the x-axis and the autonomic arousal signature on the y-axis (for similar approach see ref.[67]). As visualized in Fig. 5c, stronger weights across the whole brain (sum of squared distances to the origin [SSDO]) were observed in the non-shared Octants (1 and 5). Overall, these results suggest distinct neural representations for affective arousal

and autonomic arousal. These findings provide novel evidence for separable whole-brain fMRI multivariate patterns for the subjective experience of affective arousal and autonomic arousal, indicating functionally independent neural representations for these constructs in humans.

BAAS improves the specificity of previously established affective neural signatures

To examine whether the BAAS could enhance the specificity of previously developed affective neural signatures, we conducted a series of analyses with two signatures. The visually negative affect signatures (VNAS) was designed specifically to respond to visually induced negative affect without encompassing other forms of negative experience or more positive experiences[32]. In study 1, VNAS was capable of distinguishing negative (i.e., fear and disgust) from positive (i.e., happiness), and neutral stimuli with 76.19% and 93.65% accuracy, respectively (Fig. 6a and Table S4; for detailed descriptions of each emotional video category in study 1 see Supplementary Methods). Despite these high accuracies, the specificity of the VNAS was limited due to higher response to positive compared to neutral videos (accuracy = 75.40%, $p < 1 \times 10^{-6}$). We assessed whether incorporating arousal as control could enhance the prediction specificity of the VNAS. By adjusting for arousal rating, we found that the predictions for negative affect were maintained, with VNAS effectively distinguishing negative from positive and neutral videos, achieving 67.46% and 61.91% accuracy, respectively. Importantly, post-adjustment, the VNAS showed comparable responses to positive and neutral videos (accuracy = 51.59%, $p = 0.7894$). These findings demonstrated the potential of arousal rating regression in refining the specificity of the VNAS. Crucially, we found that adjusting the responses of the VNAS based on BAAS responses could improve prediction specificity to comparable levels, if not identical levels, to those achieved through direct arousal rating adjustments (Fig. 6a; see also Table S4). Following correction, VNAS showed comparable responses to positive and neutral videos (accuracy = 52.38%, $p = 0.6562$). Notably, the adjusted approaches also allowed the VNAS to predict negative versus positive videos more accurately than negative versus neutral videos, underscoring the utility of controlling arousal in refining prediction specificity. These findings were further replicated in study 17, where positive, negative, and neutral emotions were elicited by pictures without acquiring arousal ratings. Results consistently showed that regressing out the BAAS response enhanced the prediction specificity of the VNAS (see Supplementary Results for statistic details).

To further examine the reliability of our approach, we replicated the procedures using another affective neural signature, i.e., visually-induced disgust signature (VIDS)[13]. In study 1, VIDS predicted subjective disgust with robust discriminative power in distinguishing disgust from fear, happiness, and neutral videos, achieving 71% to 97% accuracies (Fig. 6b and Table S5). However, the VIDS also showed a heightened response to happiness (accuracy = 81.75%, $p < 1 \times 10^{-6}$) and fear (accuracy = 83.33%, $p < 1 \times 10^{-6}$) compared to neutral videos. Additionally, the VIDS exhibited a higher response to fear compared to happiness videos (accuracy = 64.29%, $p = 0.0017$). To address this issue, we incorporated adjustments for arousal ratings and BAAS responses. Following these adjustments, VIDS showed comparable responses to happiness and neutral videos, fear and neutral videos as well as fear and happiness videos (see Fig.6b and Table S5).

Collectively, our findings demonstrate the substantial potential of BAAS in refining the specificity of affective neural signatures, highlighting its prospective utility in advancing future models of affect prediction.

Discussion

Arousal represents a key dimension of the affective space and accompanies all affective experiences[68]. Despite its central role in overarching models of emotion and extensive animal models focusing on the autonomic or vigilance components or arousal a comprehensive and accurate neurofunctional model of the conscious affective experience component is lacking. Establishing such a model may allow to test whether arousal is represented independent of valence, separable from the representation of autonomic arousal and may facilitate accurate neural decoding of specific emotional states[38,40]. We combined multisensory naturalistic neuroimaging with predictive models to develop and extensively evaluate a sensitive and generalizable brain signature for affective arousal (BAAS). The signature accurately predicted affective arousal on the group and individual level in the discovery cohort and showed robust predictive performance in an independent replication sample that covered a different emotional space. The signature robustly generalized across valence domains, indicating that high affective arousal is encoded irrespective of valence in the brain. Extensive evaluation of the BAAS across 15 independent neuroimaging datasets (total n = 609) confirmed the efficacy of the BAAS in predicting affective arousal across modalities, including visual, auditory, sensory, and noxious stimulation, as well as stimulus-free anticipation periods and across valence domains, experimental paradigms, and samples, reflecting a broad generalizability of the arousal representation. The biological plausibility of the BAAS was further validated by shared common features between the BAAS and conjunction meta-analytic maps of both positive and negative affect, as derived from Neurosynth, which together with the topographic distribution of the most predictive regions of the BAAS, indicates that the amygdala, parahippocampus, PAG, and medial prefrontal systems contribute to high affective arousal across valence domains. The neural representation and predictive domain of the BAAS were moreover separable from a signature predictive of autonomic arousal, indicating that the conscious emotional experience and the autonomic components are represented in partly dissociable neural representations (in line with refs.[15,16]). Finally, and in line with the 'overshadowing' concept of high arousal overshadowing the determination of specific emotional states, we demonstrate that the BAAS can be successfully employed to considerably enhance the specificity of existing neural signatures for the target emotional state, suggesting a high application potential for the generation of more specific neuromarkers for mental processes. Together, our findings demonstrate that affective arousal can be accurately decoded from distributed brain systems encompassing both subcortical and cortical areas, with the predictive accuracy of no single region or network surpassing that of the comprehensive whole-brain model. This underscores the complexity and integrative nature of neural mechanisms underlying affective arousal[37,69]. We provide the first comprehensive neurofunctional representations of affective arousal and demonstrate that the corresponding distributed neural representation cuts across the valence domain is separable from autonomic arousal and overshadows precise decoding of specific emotional states.

The current findings revealed that affective arousal depends on the coordinated engagement of distributed representations throughout the entire brain rather than on activity in isolated brain systems, which is consistent with recent neural decoding studies demonstrating that affective processes are represented across brain systems[12-14,70]. Specifically, affective arousal experience requires concerted engagement of brain-wide distributed representations with comparable strong contributions of subcortical regions involved in affective, autonomic and motor responses to highly

salient stimuli in the environment (amygdala, parahippocampus, PAG, and caudate)[28,71-73], anterior cortical midline structures associated with global arousal and implicit emotion regulation (medial prefrontal cortex, ACC)[66,74,75], anterior insular systems involved in interoceptive and affective awareness[76,77] and sensorimotor integration (occipital cortex, SMA)[78], as well as regions that have been identified as key mediators of wakefulness and alertness in animal models (brainstem)[19,23]. Furthermore, no individual large-scale brain network (e.g., visual network, ventral attention network, and subcortical network) outperformed the BAAS in predictive performance (see Fig. 4b). Conjunction analysis revealed that the core systems (thresholded BAAS) of affective arousal are distributed across several large-scale brain networks. Notably, the DMN, ventral attention network and subcortical network exhibited significant proportions of positive predictive weights for BAAS. These findings align with previous literature suggesting that the DMN (e.g., anterior medial prefrontal cortex, portions of the ventromedial prefrontal cortex) and salience network (e.g., ACC, insula, amygdala) play crucial roles in affective arousal and conscious emotional experience[19,27,79]. From an evolutionary perspective, the engagement of these systems may facilitate the detection of salient information in the environment and trigger autonomic processes to generate the adaptive cognitive and homeostatic response[61]. Together, these findings underscore that distributed representations of affective arousal support appraisal[80] and constructionist[69] theories of emotions that propose the shared but also distinct distributed neural systems that span cortical and subcortical regions facilitate subjective affective experiences.

From a larger conceptual perspective, affective neuroscience and affective space theories propose that high affective and autonomic arousal will cut across the valence domain and characterize high-intensity positive and negative emotional experiences. In support of these conceptualizations, previous imaging meta-analysis uncovered overlapping brain regions (e.g., amygdala, striatum, thalamus, medial prefrontal cortex, ACC, and SMA) implicated in both positive and negative emotions[26], which may represent systems involved in general emotion processing (e.g. appraisal) as well as affective and autonomic arousal[5,9]. Testing the generalization of the BAAS revealed that the signature robustly decoded high positive and negative experiences to a similar extent but did not differentiate between them. Together with a flanking meta-analytic strategy identifying overlapping regions between the BAAS and both positive and negative emotional experiences, these findings indicate that the amygdala, parahippocampal gyrus, inferior and dorsomedial frontal regions code affective arousal irrespective of valence (for supporting evidence from conventional strategies see[25,26,81-83]). To further differentiate the contribution of hard-wired physiological arousal responses to the valence-independent affective arousal signature we employed a validated autonomic arousal signature and demonstrate that the BAAS has a considerably higher specificity for affective arousal. These findings are in line with a growing literature suggesting that the neural representations of the hard-wired autonomic responses and the conscious affective experience are distinguishable (for example, refs.[15,16]) and underscore that the BAAS captures the affective component.

As outlined in different domains, including subjective emotional experiences, emotion recognition as well as neural and autonomic signatures, increasing arousal progressively overshadows the characteristics of specific emotional states. From the perspective of affective neuroimaging, it is therefore critical to control for non-specific emotional processes such as arousal which is inherently associated with the affective experience[11,38,40]. We explored this conceptual and

technical perspective by employing the BAAS in combination with evaluated robust signatures for general negative affect (VNAS[32]) and disgust (VIDS[13]). In line with the overshadowing concept, the signatures showed limited specificity during immersive high-arousing emotion processing (study 1, study 17 for convergent evidence see also refs.[33,38]). While the arousal contribution considerably affects neural decoding as well as conventional affective neuroimaging experiments[84] solutions to this issue have not yet been effectively identified. We here capitalized on the BAAS to critically enhance the predictive specificity of these affective neural signatures by directly regressing out the experience of arousal. The enhanced specificity demonstrated the effectiveness of controlling for the influence of affective arousal on the prediction of emotional states. Furthermore, our findings indicate that adjusting the BAAS response yields a comparable effect to adjusting actual subjective arousal ratings. This holds particular importance given that arousal ratings are not consistently gathered in affective neuroimaging research (or the assessment can strongly interfere with the actual mental process under investigation). Our work provides a simple yet potent strategy by employing the BAAS to mitigate the impact of affective arousal, thereby significantly improving the predictive specificity of other affective neural signatures.

Some important brain systems of affective arousal are anatomically and functionally connected (e.g., amygdala and hippocampus) and some previous studies demonstrated the engagement of brain networks in wakefulness arousal fluctuations (for example, ref [85]), underscoring a potential role of brain pathways and network level communication in affective arousal[71,86] and future research may aim to deepen our understanding of the neurobiological basis of affective arousal by mapping the brain pathways that underlie this process.

In summary, we established a comprehensive distributed, generalizable, and specific predictive neural signature of affective arousal. The signature was validated and generalized across modalities, valence, paradigms, participants, and MRI systems. We showed that the neural representations of affective arousal are encoded in multiple distributed (large-scale) brain systems rather than isolated brain regions. The affective arousal signature cut across the valence domain and was distinguishable from hard-wired autonomic arousal, indicating a valence-unspecific, yet affective arousal-specific neural representation. Based on the characterization of the BAAS, we further developed a novel approach to enhancing the specificity of affective neural signatures. The current work extends our understanding of the neurobiological underpinnings of affective arousal experience and provides objective neurobiological measures of affective arousal. These measures can complement self-reported affective arousal and serve as effective supplementary tools to enhance the prediction specificity of affective models.

Methods

Overview

This research utilized data from n = 20 studies. Study 1 served as the primary study and discovery cohort, which was employed for the main analysis and development of the affective arousal signature (i.e., BAAS). Study 2 involved various emotional video stimuli to validate the identified affective arousal signatures in an independent cohort. Studies 3 to 17 comprised multiple stimuli and modalities and were utilized for the evaluation of generalizability. The autonomic arousal signature was developed in study 18 and validated in study 19. Finally, the affective arousal signature and autonomic arousal signature were compared using data from study 20. Additional

details for each study are provided in Table S1, and an overview of the main analysis is depicted in Figure 1.

Participants in study 1

Sixty-three healthy, right-handed participants were recruited from the University of Electronic Science and Technology of China (UESTC) to undergo fMRI scans during a subjective arousal rating paradigm using movie clips. All participants had no current and past physical, neurological, or psychiatric disorders and had not taken any medication in the month before the experiment. Three participants were excluded due to a lack of high arousal experience (the number of high arousal clips was less than 2, where high arousal was defined as an arousal rating score above 6), resulting in a final analysis of sixty participants (23 females; mean ± SD age = 19.55 ± 1.87 years).

The experiment procedure was approved by the local ethics committee at the University of Electronic Science and Technology of China and was conducted under the latest version of the Declaration of Helsinki. Before the regular experiments, all participants were informed that they would be shown fearful and disgusting movie clips on the screen and completed written informed consent. After the experiment, participants received monetary compensation for study participation.

Movie stimuli, arousal rating paradigm, and procedure in study 1

The movie stimuli were selected from a large pool of clips that were downloaded from an online sharing platform. This selection process was performed by two research assistants. A total of 80 movie clips, each lasts ~25s and were categorized as positive, negative, and neutral. During the pre-study, independent participants (n = 26; 10 females, age = 21.62 ± 1.92) were asked to attentively watch the clips, and rate their level of arousal, valence, and emotional consistency using a 9-point Likert scale (1 = low arousal or negative or low consistency, 9 = high arousal or positive or high consistency), and select one emotional word (such as 'fearful', 'disgusting', 'angry', 'sad', 'surprising', 'happy', 'neural', or 'ambiguous') that could accurately describe their emotional experience following each clip. The stimuli rating experiment was delivered using PsychoPy[87] version 1.85 under Windows. Low arousing neutral and high arousing positive and negative videos were selected as fMRI experiment stimuli while high emotional consistency (rating > 7) was included to serve as the reference condition.

The current study employed a within-subject design. In the arousal rating fMRI paradigm (see Fig. 1a), participants were presented with 40 arousing movie clips over 3 runs. Each run included 14 or 12 clips, which depicted humans, animals, and scenes. The order of runs and trials within a run was the same for all participants, and the order of conditions was counterbalanced before the experiment. Each video lasted approximately 25s and was followed by a white fixation cross on a black background for 1-1.2s. During the subsequent 5s period, participants were instructed to report their level of arousal during each movie using a 9-point Likert scale, where 1 indicates very low arousal and 9 indicates very high arousal. This was followed by a 10-12s wash-out period. Participants watched a total of 20 low-arousal neural movie clips, 10 high-arousal positive clips, and 10 high-arousal negative clips (details provided in Table S2). Stimulus presentation and behavioral data acquisition were controlled using MATLAB 2014a (Mathworks, Natick, MA) and Psychtoolbox (http://psychtoolbox.org/).

Before the fMRI experiment, all participants were trained on the laptop to understand the

definition of 'arousal'. After the scanning, they were asked to select the correct screenshot of movie clips presented during the fMRI experiments in a post-test.

fMRI data acquisition in study 1

fMRI data were collected using standard sequences on a 3.0-Tesla GE Discovery MR750 system (General Electric Medical System, Milwaukee, WI, USA). Structural images were acquired by using a T1-weighted MPRAGE sequence (TR = 6ms; TE = 2ms, flip angle = 9°, field of view = 256 × 256 mm^2; matrix size = 256 × 256; voxel size = 1 × 1 × 1 mm). Functional images were acquired using a T2*-weighted echo-planar sequence (TR = 2000 ms; TE = 30ms; slices = 39; flip angle = 90°; field of view = 240 × 240 mm; matrix size = 64 × 64, voxel size: 3.75 × 3.75 × 4 mm).

Participants in study 2

A total of 38 healthy right-handed UESTC students were initially recruited for the study. Following exclusion criteria based on low arousal ratings for positive or negative videos in the fMRI experiments, 36 subjects (17 female, mean ± SD age = 21.03 ± 2.22) were enrolled in the final analysis. All participants were free of current and past physical, neurological, or psychiatric disorders and had no contraindications for MRI. Provided written informed consent before participation and the experimental procedures were approved by the local ethics committee at UESTC, in accordance with the latest version of the Declaration of Helsinki. Monetary compensation was provided to all participants for their participation in the study.

Movie stimuli, arousal rating paradigm in study 2

Thirty-one movie clips (~60s duration of each) were selected by two researchers. An independent sample of 52 participants (32 females, mean ± SD age = 21.00 ± 2.51) reported the valence, arousal, emotional consistency, and emotional experience ('fearful', 'disgusting', 'sad', 'ambiguous negative', 'happy', 'exciting', 'romantic', 'ambiguous positive', and 'neutral') while watching each video. Of note, when participants had multiple positive or negative emotions, the labels 'ambiguous positive' or 'ambiguous negative' were chosen (e.g., if a video evokes both happiness and excitement). The selected fMRI video stimuli were chosen based on the results of the behavioral experiment as (1) they were rated high emotional consistency (rating > 7) and (2) their core emotional experience was accurately described (i.e., no positive videos labeled with negative emotions, and no negative videos labeled with positive emotions).

In the arousal rating fMRI paradigm, there were a total of 28 one-minute videos. These videos represented two affective states (9 positive clips and 9 negative clips) as well as a neutral state (10 neutral clips). More details can be found in Table S2. During fMRI, all stimuli were presented in three runs, with either three or four clips from each category in each run. The fMRI paradigm used in the validation cohort was the same as the one used in the discovery cohort, except for differences in the presentation time settings for the stimuli.

fMRI data acquisition in study 2

fMRI data were collected on a 3.0-Tesla GE Discovery MR750 system (General Electric Medical System, Milwaukee, WI, USA). Functional images were acquired using a T2*-weighted echo-planar sequence (TR = 2000ms; TE = 30ms; slices = 36; flip angle = 90°; field of view = 200 × 200 mm^2; matrix size = 64 × 64, voxel size: 3.125 × 3.125 × 3.8 mm). To improve spatial normalization and

exclude subjects with apparent brain pathologies structural images were acquired by using a T1-weighted MPRAGE sequence (TR = 8ms; TE =3ms, flip angle = 8°, field of view = 256 × 256 mm; matrix size = 256 × 256; voxel size = 1 × 1 × 1 mm).

fMRI data preprocessing in studies 1 and 2

Before the automated preprocessing, the first 4 volumes of each run were removed to stabilize image intensity. Imaging data were preprocessed using FMRIPREP 21.0.0(RRID: SCR_016216; https://github.com/nipreps/fmriprep)[88], a Nipype 1.6.156 based tool that integrates preprocessing routines from different software packages, including slice time corrected (using 3dTshif from AFNI), motion correction (using mcflirt from FSL v6.0.5.1), brain tissue segmentation of cerebrospinal fluid (CSF), white matter, and gray matter (using FAST from FSL v6.0.5.1), coregistration (using boundary-Based registration with six degrees of freedom from FLIRT), and affine transformation of the functional volumes to the 2 mm isotropic T1w anatomical and subsequently to MNI space (using ANTs v2.3.3). To perform denoising, we fit a voxel-wise general linear model (GLM) for each participant. Specifically, in line with the ref[89], we removed variance associated with the mean, linear and quadratic trends, the average signal within anatomically-derived eroded CSF mask, the effects of motion estimated during the head-motion correction using an expanded set of 24 motion parameters (six realignment parameters, their squares, their derivatives, and their squared derivatives) and motion spikes (FMRIPREP default: framewise displacement (FD) > 0.5mm or standardized DVARS > 1.5). For arousal rating data we additionally constructed a task-related regressor with rating period convolved with canonical hemodynamic response function (HRF).

Data averaging

To develop the subjective affective arousal signatures, we first generated arousal-related activation features for each subject. For each participant, we concatenated the fMRI data with the same arousal level rating during the stimuli presentation period. Notably, the onset time for each video was shifted by 2-3 TRs due to the hemodynamic lag. Next, we calculated the voxel-wise mean activation for each arousal level and each subject separately. For the single-trial analysis, we also acquired the fMRI data for each stimulus. The same method was employed for the fMRI data collected in study 2.

Brain affective arousal signature development and evaluation

In study 1, we developed a predictive model of arousal ratings based on whole-brain activation (i.e., BAAS). Whole-brain data mask with gray matter from this study was used. We employed the support vector regression (SVR) algorithm using a linear kernel (C=1) implemented in the Spider toolbox (http://people.kyb.tuebingen.mpg.de/spider) with voxel-wise activation maps from each rating as the predictor (true arousal ratings as outcome). We employed a 10×10-fold cross-validation procedure to evaluate the identified signature, which involved random assignment of all participants to 10 subsamples, comprising 6 individuals, using MATLAB's cvpartition function. The optimal hyperplane was then derived from the multivariate pattern observed in the training set, consisting of 54 participants, and subsequently evaluated using the excluded 6 participants in the test set. This rigorous procedure was repeated ten times, with each subsample serving as the testing set once. To thoroughly evaluate the neurofunctional signature, we employed a range of robust metrics including prediction-outcome correlation, the average root mean squared error (RMSE), and the coefficient

of determination (R^2). Specifically, we estimated the Pearson correlation (r) between cross-validation predicted and observed ratings (that is, true arousal ratings) to indicate the effect sizes, including overall (between and within-subject; 396 pairs in total) and within-subject Pearson correlation coefficient. RMSE illustrated the overall prediction errors, while R^2 represented the percentage of arousal rating variance accounted for by the prediction models. The formula is:

$$R^2 = 1 - \frac{\sum_{i=1}^{n}(y_i - \hat{y}_i)^2}{\sum_{i=1}^{n}(y_i - \bar{y})^2}$$

where y_i is the true arousal rating for the i-th sample, $\hat{y}_i$ is the model predicted rating for the i-th sample, and $\bar{y}$ is the mean of all arousal ratings.

To further evaluate the performance of the arousal-predictive pattern (trained on the discovery cohort), we applied BAAS to validation and generalization datasets. In the validation cohort (study 2), signature responses were calculated by taking the dot product of the BAAS weight map with the test images for each participant for each arousal level. The overall and within-subject Pearson correlation coefficient, RMSE, and R^2 between the predicted and observed ratings were used to determine the performance. Furthermore, we evaluated the performance of BAAS in predicting different levels of arousal experience in the validation cohort by assessing classification accuracies using a forced-choice test. The intensity of affective arousal was classified into three levels: low intensity (1-3 scores), medium intensity (4-6 scores), and high intensity (7-9 scores). We compared the distinctive responses under two different conditions for each level of intensity (low versus medium, medium versus high, low versus high), and considered the condition with the higher signature response as being more associated with increased affective arousal experience. To determine the specificity of the neural signature for affective arousal rather than valence, we also computed the classification accuracies of the BAAS pattern using a two-forced-choice test. This involved comparing the signature responses for positive and negative conditions within the same individual.

Within-subject trial-wise prediction

After evaluating the performance of BAAS in predictions of 'average' arousal ratings, we tested whether BAAS could effectively predict individual trial-by-trial subjective arousal levels. To this end, we performed a single-trial analysis[13,14]. Specifically, we calculated the BAAS pattern expressions of single-trial voxel-wise activation maps for each participant in the discovery cohort, which involved taking the dot-product of vectorized activation images with the BAAS weights. We then correlated the pattern expressions with the true ratings separately for each participant. Of note, we used the 10×10 fold cross-validation procedure to obtain the BAAS response of each single-trial activation map for each subject in the discovery cohort, and did not exclude any trials in this analysis.

Generalization of BAAS performance

To evaluate the generalizability of the arousal signature, we examined its response in fifteen independent datasets from opening research (details see Table S1). In studies 3 - 6 and study 17, we assessed classification accuracies of BAAS between high and low arousal feelings induced by various emotional stimuli and modalities using a two-alternative forced-choice method based on the pattern expressions (i.e., the dot-product of BAAS weight map and test image plus the intercept). In studies 7 – 16, we conducted a one-sample t-test to examine whether there existed significant

differences between BAAS responses (via dot-produts) for positive and baseline contrasts.

Identifying neurofunctional characterization of affective arousal

We performed a comprehensive analysis to identify the core brain regions (i.e., having voxels that reliably contribute to model weights) associated with subjective affective arousal processes. To this end, we conducted a bootstrap test using 5,000 samples with replacements from the discovery cohort to determine the voxels that made the most reliable contribution to the prediction and calculated Z-scores at each voxel with the mean and standard deviation of the sampling distribution. The resulting maps were thresholded voxel-wise at $q < 0.05$ (FDR corrected). To evaluate the validity and neurobiological plausibility of core systems, we additionally employed the following analyses to identify the specific neural basis underlying the subjective experience of affective arousal: (1) Based on previous studies[13,14], we performed multivariate analyses to obtain within-subject models. We then conducted a one-sample t-test (thresholded at $q < 0.05$, FDR corrected) to identify brain regions significantly related to affective arousal processing (see Supplementary Methods for detailed methods). (2) We obtained first-level univariate parametric modulation beta maps and performed a one-sample t-test on all images to identify regions of activation associated with arousal ratings. (3) We compared the BAAS with the conjunction of 'positive affect' and 'negative affect' Neurosynth maps (association test $q < 0.05$, FDR corrected; 'positive affect' studies n = 1,095; 'negative affect' studies n = 769) to confirm the biological plausibility of core systems. Overall, these analyses provide an extensive assessment of the neurobiological basis of the subjective experience of affective arousal.

To evaluate whether affective arousal processing, as a component of 'core affect', could be characterized by activations within a single network or if it is neurobiologically supported by large-scale networks, as proposed by psychological construction theories[26], we compared the prediction performances of large-scale networks against whole brain approaches. The networks of interest included seven resting-state functional networks and a subcortical network, including amygdala, hippocampus, striatum, and thalamus (from Brainnetome atlas[90]). To conduct this analysis, we trained and tested the model for the network using discovery data with a 10×10-fold cross-validation method. As the experience of affective arousal was distributed across multiple neural systems and supported by large-scale networks (see results), we created a polar plot to illustrate the proportion of overlaps between core systems (thresholded BAAS) against a set of anatomical parcellations (seven resting-state functional networks and one subcortical network). To reduce potential biases arising from different atlases, we continued to use the Brainnetome atlas.

Comparing the affective arousal signature and autonomic arousal signature

Previous literature has highlighted the potential distinction between affective arousal and autonomic arousal[19]. To compare these, we trained a whole-brain autonomic arousal decoder in the study 18 (n = 25). Detailed information about the data and training methods for study 18 is provided in the Supplementary Methods. This decoder was also applied to study 19 (n = 58), where we assessed the two-alternative forced-choice classification accuracy between CS+ (associated with high SCL) and CS- (associated with low SCL) to validate the reliability of the identified autonomic arousal signature. Subsequently, the differences between the BAAS and the autonomic arousal signature were determined by: (1) calculating the two-alternative forced-choice classification accuracies between different anxious arousal intensity levels (as well as SCL) based on pattern expression in

study 20 (details of this study see Supplementary Methods), and (2) plotting the joint distribution of normalized whole-brain weights of affective arousal and autonomic arousal patterns (see Supplementary Methods for details).

Evaluating the potential of BAAS in enhancing the specificity of affective neural signatures

Previous studies have developed and evaluated whole-brain affective decoders for general negative affect experience (VNAS[32], from another lab) and subjective disgust experience (VIDS[13], from our lab). To evaluate the potential of BAAS in improving the specificity of affective neural signatures, we conducted a series of analyses. Firstly, VNAS were applied to evaluate responses to a collection of emotional videos, including negative (i.e., fear and disgust), positive (i.e., happiness) and neutral emotions in study 1. We quantified the pattern responses (i.e., the dot-product of model and test brain activation map) and assessed the predictive accuracies using a single-interval classification. This method for estimating neural response patterns was consistently applied in subsequent analyses. Secondly, we examined whether controlling for arousal ratings in VNAS predictions could enhance specificity. Specifically, we used BAAS to predict the arousal scores of each subject during each category of emotional experience. After regressing out the predicted arousal scores from VNAS responses across all conditions, we reevaluated the predictive performances of the VNAS under each condition. Finally, we examined the predictive accuracy of VNAS after adjusting their responses based on the BAAS responses. This involved obtaining the BAAS response for each condition and then controlling for these BAAS responses in the VNAS responses across all conditions. We also validated these findings in study 17. Specifically, we tested testing whether adjusting the VNAS responses based on BAAS responses could enhance the predictive specificity of the VNAS when the dataset did not include any arousal ratings. To further validate our findings, we employed another affective neural signature, i.e., VIDS. In study 1, VIDS was used to predict responses to disgust, fear, happiness, and neutral videos, following the same analysis pipeline as described above.

Behavioral data analysis

We used MATLAB script to check all behavioral data and exclude the participants who had a low affective experience. Statistical analyses of behavioral data were carried out using SPSS software (version 22; IBM Corp., Armonk, NY). We examined whether participants had strong arousal during the stimuli presentation (details see results).

Acknowledgments

We thank J.X. He, D. Liu, and K. Fu for assisting in data collection; M. Čeko and colleagues for sharing data included in study 4; T. Wager and colleagues for sharing data included in study 5; X.Q. Liu and colleagues for sharing data included in study 6 and study 20; P. Kragel and colleagues for sharing data included in studies 7 – 16; D.C., D.J.-F.d.Q and colleagues for sharing data included in study 17; V. Taschereau-Dumouchel and colleagues for sharing data included in study 18. Any opinions, findings, conclusions, or recommendations expressed in this publication do not reflect the views of the Government of the Hong Kong Special Administrative Region or the Innovation and Technology Commission. This work was partly supported by the National Natural Science Foundation of China (grant nos. 32250610208 and 82271583 to B.B., and 32300862 to F.Z.), National Key Research and Development Program of China (grant no. 2018YFA0701400) to B.B.,

the Natural Science of Foundation of Chongqing (CSTB2023NSCQ-MSX0889) to F.Z. and a start-up grant from the University of Hong Kong to B.B.

Author contributions

R.Z., F.Z., and B.B. conceived and designed the experiment. R.Z., G. J., and F.Z. selected the videos of studies 1 and 2. R.Z., X.G., and L.W. collected the data for studies 1 and 2. R.Z. preprocessed the data for studies 1 and 2. R.Z., F.Z., and B.B. analyzed the data and were responsible for the interpretation of the data. X.G., T.X., F.Y., and X.S. provided important suggestions during the formal analysis. R.Z. drafted the manuscript. X.G. and T.X. provided suggestions during manuscript writing. F.Z. and B.B. revised the paper. B.B. supervised the project.

Competing interests

The authors declare no competing interests.

References

1 Chikazoe, J., Lee, D. H., Kriegeskorte, N. & Anderson, A. K. Population coding of affect across stimuli, modalities and individuals. *Nature neuroscience* **17**, 1114-1122 (2014).

2 Harmon-Jones, E., Harmon-Jones, C. & Summerell, E. On the importance of both dimensional and discrete models of emotion. *Behavioral sciences* **7**, 66 (2017).

3 Russell, J. A. Core affect and the psychological construction of emotion. *Psychological review* **110**, 145 (2003).

4 Yik, M. S., Russell, J. A. & Barrett, L. F. Structure of self-reported current affect: Integration and beyond. *Journal of personality and social psychology* **77**, 600 (1999).

5 Russell, J. A. A circumplex model of affect. *Journal of personality and social psychology* **39**, 1161 (1980).

6 Remington, N. A., Fabrigar, L. R. & Visser, P. S. Reexamining the circumplex model of affect. *Journal of personality and social psychology* **79**, 286 (2000).

7 Anderson, D. J. & Adolphs, R. A framework for studying emotions across species. *Cell* **157**, 187-200 (2014).

8 Kuppens, P. *et al.* The relation between valence and arousal in subjective experience varies with personality and culture. *Journal of personality* **85**, 530-542 (2017).

9 Kuppens, P., Tuerlinckx, F., Russell, J. A. & Barrett, L. F. The relation between valence and arousal in subjective experience. *Psychological bulletin* **139**, 917 (2013).

10 Holz, N., Larrouy-Maestri, P. & Poeppel, D. The paradoxical role of emotional intensity in the perception of vocal affect. *Scientific reports* **11**, 9663 (2021).

11 Wager, T. D., Krishnan, A., Hitchcock, E. & Wager, T. D. How are emotions organized in the brain. *The nature of emotion. Fundamental questions*, 112-118 (2018).

12 Chang, L. J., Gianaros, P. J., Manuck, S. B., Krishnan, A. & Wager, T. D. A sensitive and specific neural signature for picture-induced negative affect. *PLoS biology* **13**, e1002180 (2015).

13 Gan, X. *et al.* A neurofunctional signature of subjective disgust generalizes to oral distaste and socio-moral contexts. *Nature Human Behaviour*, 1-20 (2024).

14 Zhou, F. *et al.* A distributed fMRI-based signature for the subjective experience of fear. *Nature communications* **12**, 6643 (2021).

15 Taschereau-Dumouchel, V., Kawato, M. & Lau, H. Multivoxel pattern analysis reveals dissociations between subjective fear and its physiological correlates. *Molecular psychiatry* **25**,

2342-2354 (2020).
16 Liu, X. *et al.* A neural signature for the subjective experience of threat anticipation under uncertainty. *Nature Communications* **15**, 1544 (2024).
17 Dewey, J. The theory of emotion: I: emotional attitudes. *Psychological review* **1**, 553 (1894).
18 Schachter, S. & Singer, J. Cognitive, social, and physiological determinants of emotional state. *Psychological review* **69**, 379 (1962).
19 Satpute, A. B., Kragel, P. A., Barrett, L. F., Wager, T. D. & Bianciardi, M. Deconstructing arousal into wakeful, autonomic and affective varieties. *Neuroscience letters* **693**, 19-28 (2019).
20 Paxinos, G. & Watson, C. *The rat brain in stereotaxic coordinates: hard cover edition*. (Elsevier, 2006).
21 Fuller, P., Sherman, D., Pedersen, N. P., Saper, C. B. & Lu, J. Reassessment of the structural basis of the ascending arousal system. *Journal of Comparative Neurology* **519**, 933-956 (2011).
22 Adolphs, R., Damasio, A. R. & Borod, J. Neurobiology of emotion at a systems level. *The neuropsychology of emotion*, 194-213 (2000).
23 Parvizi, J. & Damasio, A. Consciousness and the brainstem. *Cognition* **79**, 135-160 (2001).
24 Saper, C. B., Fuller, P. M., Pedersen, N. P., Lu, J. & Scammell, T. E. Sleep state switching. *Neuron* **68**, 1023-1042 (2010).
25 Hofmann, S. M. *et al.* Decoding subjective emotional arousal from EEG during an immersive virtual reality experience. *Elife* **10**, e64812 (2021).
26 Lindquist, K. A., Satpute, A. B., Wager, T. D., Weber, J. & Barrett, L. F. The brain basis of positive and negative affect: evidence from a meta-analysis of the human neuroimaging literature. *Cerebral cortex* **26**, 1910-1922 (2016).
27 Phan, K. L., Wager, T., Taylor, S. F. & Liberzon, I. Functional neuroanatomy of emotion: a meta-analysis of emotion activation studies in PET and fMRI. *Neuroimage* **16**, 331-348 (2002).
28 Buhle, J. T. *et al.* Common representation of pain and negative emotion in the midbrain periaqueductal gray. *Social cognitive and affective neuroscience* **8**, 609-616 (2013).
29 Shamay-Tsoory, S. G. & Mendelsohn, A. Real-life neuroscience: an ecological approach to brain and behavior research. *Perspectives on Psychological Science* **14**, 841-859 (2019).
30 Poldrack, R. A. *et al.* Scanning the horizon: towards transparent and reproducible neuroimaging research. *Nature reviews neuroscience* **18**, 115-126 (2017).
31 Elliott, M. L. *et al.* What is the test-retest reliability of common task-functional MRI measures? New empirical evidence and a meta-analysis. *Psychological science* **31**, 792-806 (2020).
32 Čeko, M., Kragel, P. A., Woo, C.-W., López-Solà, M. & Wager, T. D. Common and stimulus-type-specific brain representations of negative affect. *Nature neuroscience* **25**, 760-770 (2022).
33 Zhou, F. *et al.* Empathic pain evoked by sensory and emotional-communicative cues share common and process-specific neural representations. *elife* **9**, e56929 (2020).
34 Kragel, P. A., Koban, L., Barrett, L. F. & Wager, T. D. Representation, pattern information, and brain signatures: from neurons to neuroimaging. *Neuron* **99**, 257-273 (2018).
35 Kragel, P. A., Han, X., Kraynak, T. E., Gianaros, P. J. & Wager, T. D. Functional MRI can be highly reliable, but it depends on what you measure: A commentary on Elliott et al.(2020). *Psychological Science* **32**, 622-626 (2021).
36 Woo, C.-W., Chang, L. J., Lindquist, M. A. & Wager, T. D. Building better biomarkers: brain models in translational neuroimaging. *Nature neuroscience* **20**, 365-377 (2017).
37 Lindquist, K. A., Wager, T. D., Kober, H., Bliss-Moreau, E. & Barrett, L. F. The brain basis of

emotion: a meta-analytic review. *Behavioral and brain sciences* **35**, 121-143 (2012).

38 Zhou, F. *et al.* Capturing dynamic fear experiences in naturalistic contexts: An ecologically valid fMRI signature integrating brain activation and connectivity. *bioRxiv*, 2023.2008. 2018.553808 (2023).

39 Kohoutová, L. *et al.* Individual variability in brain representations of pain. *Nature neuroscience* **25**, 749-759 (2022).

40 Kragel, P. A. & LaBar, K. S. Decoding the nature of emotion in the brain. *Trends in cognitive sciences* **20**, 444-455 (2016).

41 Barrett, L. F. Are emotions natural kinds? *Perspectives on psychological science* **1**, 28-58 (2006).

42 Yarkoni, T., Poldrack, R. A., Nichols, T. E., Van Essen, D. C. & Wager, T. D. Large-scale automated synthesis of human functional neuroimaging data. *Nature methods* **8**, 665-670 (2011).

43 Liberzon, I., Phan, K. L., Decker, L. R. & Taylor, S. F. Extended amygdala and emotional salience: a PET activation study of positive and negative affect. *Neuropsychopharmacology* **28**, 726-733 (2003).

44 Mourao-Miranda, J. *et al.* Contributions of stimulus valence and arousal to visual activation during emotional perception. *Neuroimage* **20**, 1955-1963 (2003).

45 Britton, J. C., Taylor, S. F., Sudheimer, K. D. & Liberzon, I. Facial expressions and complex IAPS pictures: common and differential networks. *Neuroimage* **31**, 906-919 (2006).

46 Gan, X. *et al.* Common and distinct neurofunctional representations of core and social disgust in the brain: Coordinate-based and network meta-analyses. *Neuroscience & Biobehavioral Reviews* **135**, 104553 (2022).

47 Kuppens, P., Oravecz, Z. & Tuerlinckx, F. Feelings change: accounting for individual differences in the temporal dynamics of affect. *Journal of personality and social psychology* **99**, 1042 (2010).

48 Mikutta, C., Altorfer, A., Strik, W. & Koenig, T. Emotions, arousal, and frontal alpha rhythm asymmetry during Beethoven's 5th symphony. *Brain topography* **25**, 423-430 (2012).

49 Wager, T. D. *et al.* An fMRI-based neurologic signature of physical pain. *New England Journal of Medicine* **368**, 1388-1397 (2013).

50 Kragel, P. A. & LaBar, K. S. Multivariate neural biomarkers of emotional states are categorically distinct. *Social cognitive and affective neuroscience* **10**, 1437-1448 (2015).

51 Lepping, R. J. *et al.* Neural processing of emotional musical and nonmusical stimuli in depression. *PloS one* **11**, e0156859 (2016).

52 Iranpour, J., Morrot, G., Claise, B., Jean, B. & Bonny, J.-M. Using high spatial resolution to improve BOLD fMRI detection at 3T. *PLoS One* **10**, e0141358 (2015).

53 Smeets, P. A., Kroese, F. M., Evers, C. & de Ridder, D. T. Allured or alarmed: counteractive control responses to food temptations in the brain. *Behavioural brain research* **248**, 41-45 (2013).

54 Tom, S. M., Fox, C. R., Trepel, C. & Poldrack, R. A. The neural basis of loss aversion in decision-making under risk. *Science* **315**, 515-518 (2007).

55 Laurent, H. K., Wright, D. & Finnegan, M. Mindfulness-related differences in neural response to own infant negative versus positive emotion contexts. *Developmental cognitive neuroscience* **30**, 70-76 (2018).

56 Tomova, L. *et al.* Acute social isolation evokes midbrain craving responses similar to hunger. *Nature neuroscience* **23**, 1597-1605 (2020).

57 Dalenberg, J. R., Weitkamp, L., Renken, R. J. & Ter Horst, G. J. Valence processing differs across stimulus modalities. *NeuroImage* **183**, 734-744 (2018).

58 Kragel, P. A., Reddan, M. C., LaBar, K. S. & Wager, T. D. Emotion schemas are embedded in the human visual system. *Science advances* **5**, eaaw4358 (2019).

59 Castrellon, J. J. *et al.* Mesolimbic dopamine D2 receptors and neural representations of subjective value. *Scientific reports* **9**, 20229 (2019).

60 Fastenrath, M. *et al.* Human cerebellum and corticocerebellar connections involved in emotional memory enhancement. *Proceedings of the National Academy of Sciences* **119**, e2204900119 (2022).

61 Menon, V. & Uddin, L. Q. Saliency, switching, attention and control: a network model of insula function. *Brain structure and function* **214**, 655-667 (2010).

62 Zheng, J. *et al.* Amygdala-hippocampal dynamics during salient information processing. *Nature communications* **8**, 14413 (2017).

63 Amting, J. M., Greening, S. G. & Mitchell, D. G. Multiple mechanisms of consciousness: the neural correlates of emotional awareness. *Journal of neuroscience* **30**, 10039-10047 (2010).

64 Richardson, M. P., Strange, B. A. & Dolan, R. J. Encoding of emotional memories depends on amygdala and hippocampus and their interactions. *Nature neuroscience* **7**, 278-285 (2004).

65 Jacobs, S. C. *et al.* Use of skin conductance changes during mental stress testing as an index of autonomic arousal in cardiovascular research. *American heart journal* **128**, 1170-1177 (1994).

66 Zhou, F. *et al.* Human extinction learning is accelerated by an angiotensin antagonist via ventromedial prefrontal cortex and its connections with basolateral amygdala. *Biological psychiatry* **86**, 910-920 (2019).

67 Koban, L., Jepma, M., López-Solà, M. & Wager, T. D. Different brain networks mediate the effects of social and conditioned expectations on pain. *Nature communications* **10**, 1-13 (2019).

68 Schiller, D. *et al.* The human affectome. *Neuroscience & Biobehavioral Reviews* **158**, 105450 (2024).

69 Barrett, L. F. The theory of constructed emotion: an active inference account of interoception and categorization. *Social cognitive and affective neuroscience* **12**, 1-23 (2017).

70 Kragel, P. A., Treadway, M. T., Admon, R., Pizzagalli, D. A. & Hahn, E. C. A mesocorticolimbic signature of pleasure in the human brain. *Nature Human Behaviour* **7**, 1332-1343 (2023).

71 Fastenrath, M. *et al.* Dynamic modulation of amygdala–hippocampal connectivity by emotional arousal. *Journal of neuroscience* **34**, 13935-13947 (2014).

72 Kilpatrick, L. & Cahill, L. Amygdala modulation of parahippocampal and frontal regions during emotionally influenced memory storage. *Neuroimage* **20**, 2091-2099 (2003).

73 Mihov, Y. *et al.* Mirroring fear in the absence of a functional amygdala. *Biological psychiatry* **73**, e9-11, doi:10.1016/j.biopsych.2012.10.029 (2013).

74 Ridderinkhof, K. R., Ullsperger, M., Crone, E. A. & Nieuwenhuis, S. The role of the medial frontal cortex in cognitive control. *science* **306**, 443-447 (2004).

75 Mashour, G. A., Pal, D. & Brown, E. N. Prefrontal cortex as a key node in arousal circuitry. *Trends in neurosciences* **45**, 722-732, doi:10.1016/j.tins.2022.07.002 (2022).

76 Craig, A. D. How do you feel--now? The anterior insula and human awareness. *Nature reviews. Neuroscience* **10**, 59-70, doi:10.1038/nrn2555 (2009).

77 Li, Y. *et al.* Linking brain structure and activation in anterior insula cortex to explain the trait empathy for pain. *Human brain mapping* **41**, 1030-1042 (2020).

78 Palva, S. & Palva, J. M. Roles of brain criticality and multiscale oscillations in temporal predictions for sensorimotor processing. *Trends in neurosciences* **41**, 729-743 (2018).

79 Ince, S. *et al.* Subcortical contributions to salience network functioning during negative emotional processing. *NeuroImage* **270**, 119964 (2023).

80 Clore, G. L. & Ortony, A. Appraisal theories: How cognition shapes affect into emotion. (2008).

81 Kim, S. H. & Hamann, S. Neural correlates of positive and negative emotion regulation. *Journal of cognitive neuroscience* **19**, 776-798 (2007).

82 Garavan, H., Pendergrass, J. C., Ross, T. J., Stein, E. A. & Risinger, R. C. Amygdala response to both positively and negatively valenced stimuli. *Neuroreport* **12**, 2779-2783 (2001).

83 Hamann, S. & Mao, H. Positive and negative emotional verbal stimuli elicit activity in the left amygdala. *Neuroreport* **13**, 15-19 (2002).

84 Ferraro, S. *et al.* The central autonomic system revisited–convergent evidence for a regulatory role of the insular and midcingulate cortex from neuroimaging meta-analyses. *Neuroscience & Biobehavioral Reviews* **142**, 104915 (2022).

85 Damaraju, E., Tagliazucchi, E., Laufs, H. & Calhoun, V. D. Connectivity dynamics from wakefulness to sleep. *Neuroimage* **220**, 117047, doi:10.1016/j.neuroimage.2020.117047 (2020).

86 Wang, L. *et al.* Arousal modulates the amygdala-insula reciprocal connectivity during naturalistic emotional movie watching. *Neuroimage* **279**, 120316 (2023).

87 Peirce, J. W. PsychoPy—psychophysics software in Python. *Journal of neuroscience methods* **162**, 8-13 (2007).

88 Esteban, O. *et al.* fMRIPrep: a robust preprocessing pipeline for functional MRI. *Nature methods* **16**, 111-116 (2019).

89 Chang, L. J. *et al.* Endogenous variation in ventromedial prefrontal cortex state dynamics during naturalistic viewing reflects affective experience. *Science Advances* **7**, eabf7129 (2021).

90 Fan, L. *et al.* The human brainnetome atlas: a new brain atlas based on connectional architecture. *Cerebral cortex* **26**, 3508-3526 (2016).

Tables and Figures

Table 1. Generalization performance of the BAAS on studies 7– 16

Study index	Comparison	*t*	*p* value
7	*Pleasant music vs baseline*	2.81	0.0084
8	*Pleasant music vs baseline*	2.62	0.0170
9	*Appetitive food vs baseline*	2.72	0.0141
10	*Appetitive food vs baseline*	6.41	$< 1\times10^{-6}$
11	*Reward cues vs baseline*	3.36	0.0072
12	*Parametric modulation of reward*	8.46	$< 1\times10^{-6}$
13	*Videos of own baby vs baseline*	3.30	0.0031
14	*Social images vs baseline*	1.97	0.0681
15	*Erotic images vs baseline*	2.46	0.0222
16	*Erotic images vs baseline*	6.21	$< 1\times10^{-6}$

BAAS, Brain affective arousal signature.

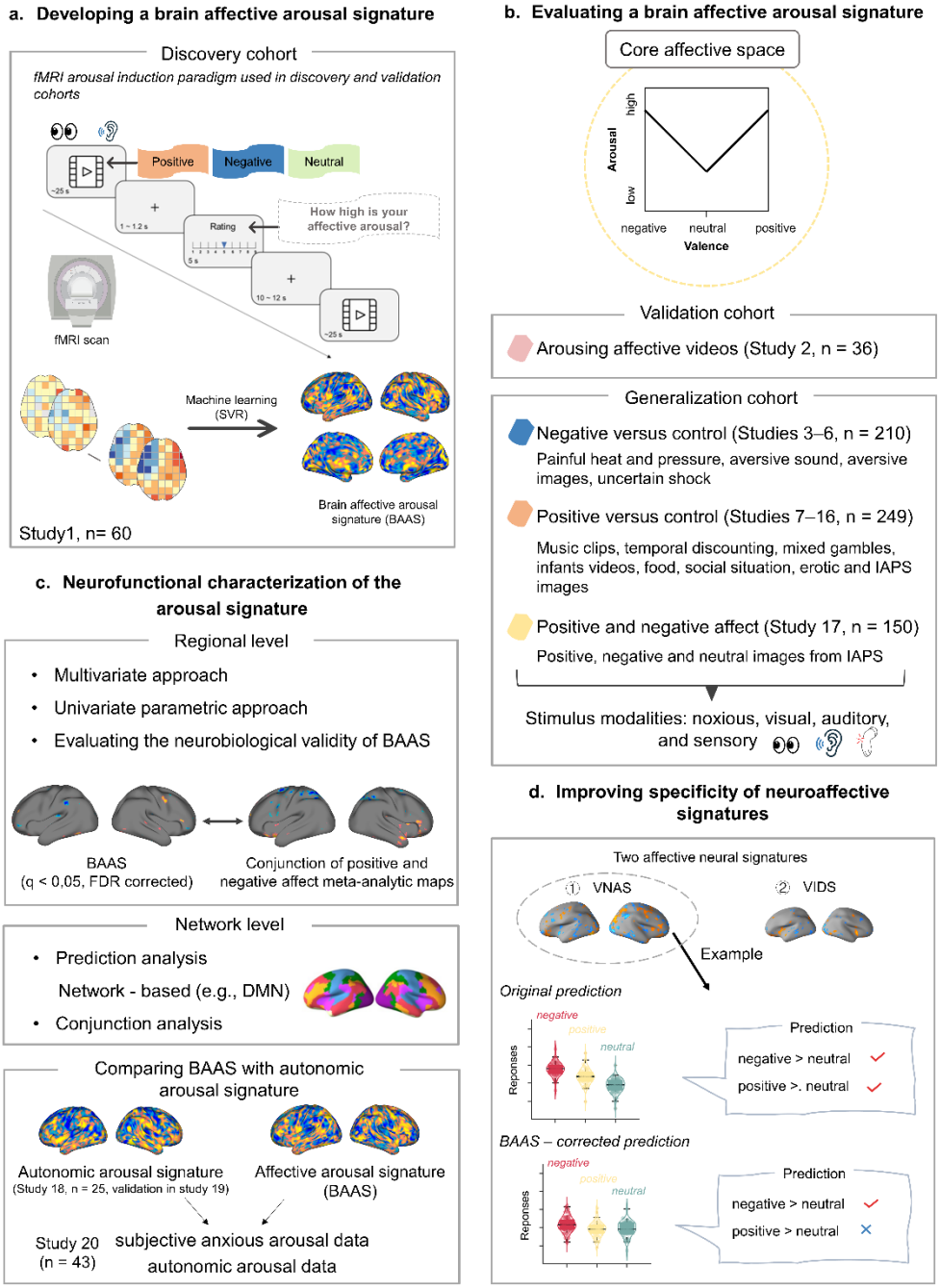

Fig. 1 Experimental paradigm and main analyses. (**a**) Building a brain affective arousal signature. A whole-brain model (brain affective arousal signature, BAAS) was developed on the discovery cohort that underwent an arousal induction fMRI paradigm (study 1, n = 60) using the support vector regression algorithm. (**b**) Evaluating the brain affective arousal signature. Based on the dimensional models of 'core affect', BAAS was evaluated in the validation (study 2, n = 36) and generalization (studies 3 – 17, n = 609) cohorts. (**c**) Identifying the neurofunctional representation of affective arousal in the brain. Multivariate and univariate approaches were employed to determine the contribution of specific brain systems to predict subjective affective arousal. To validate the biological plausibility of the identified affective arousal brain systems, the thresholded affective arousal signature was compared with the conjunction of meta-analytic maps for positive and

negative affect. The performance of isolated systems (i.e., single network) in predicting affective arousal experiences and the differences between affective arousal and autonomic arousal signatures were evaluated to validate existed arousal-related domains. (**d**) Improving the specificity of neuroaffective signatures. Testing the specificity of two affective neural signatures (VNAS and VIDS) before and after BAAS response corrected. VANS, visually negative affect signature from Čeko et al[32]. VIDS, visually induced disgust signature from Gan et al[13].

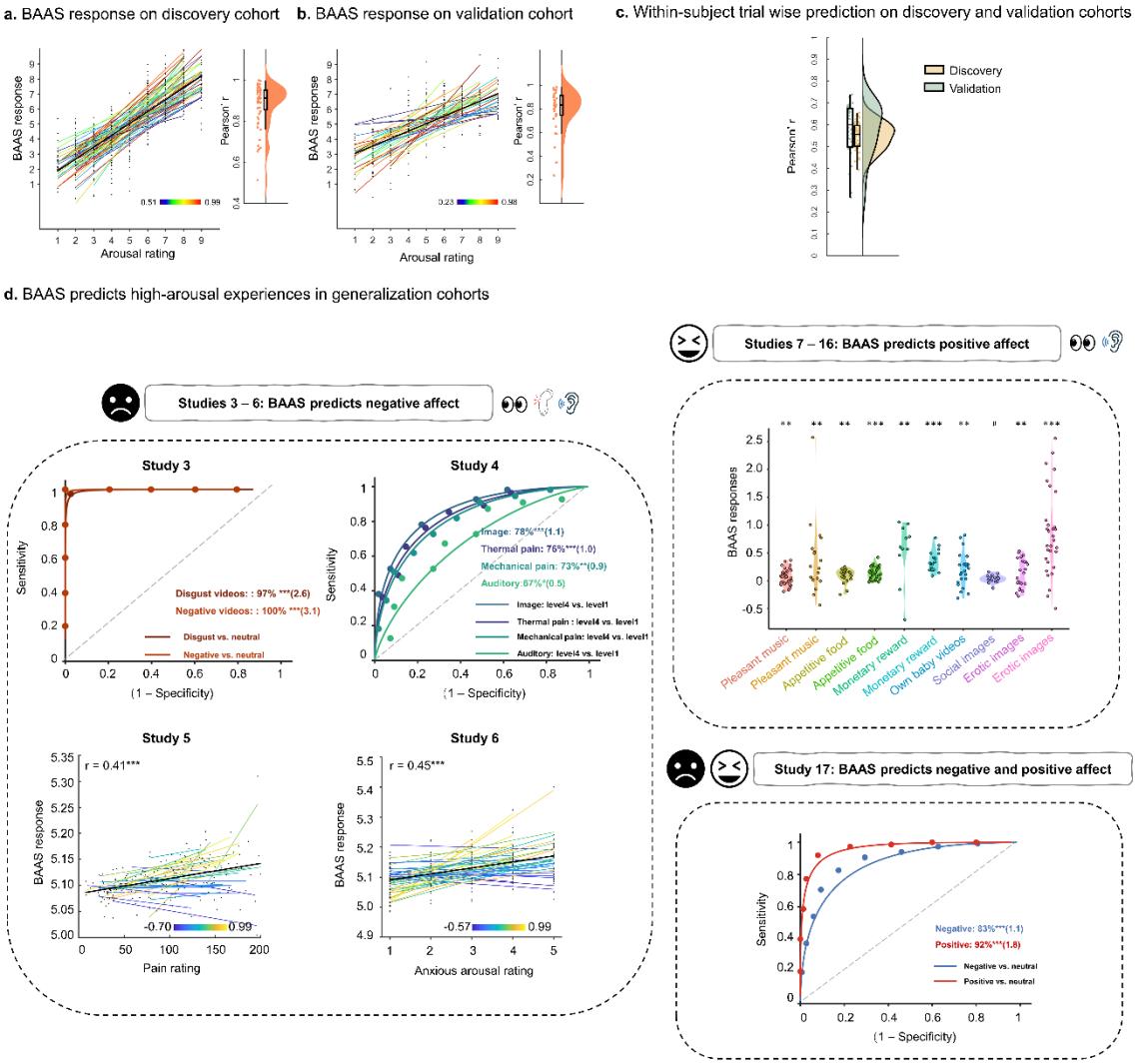

Fig. 2 Evaluating the Brain Affective Arousal Signature (BAAS). (**a**) and (**b**) depict predicted arousal experience compared to the actual level of arousal for the cross-validated discovery cohort (study 1, n = 60) and the independent validation cohort (study 2, n = 36), respectively. Colored lines indicate the Pearson correlation coefficients between predicted and true ratings in each subject. The black line reflects the overall correlation. Raincloud plots show the distribution of correlation. (**c**) Distribution of within-subject trial-wise prediction-outcome correlation coefficients for each participant in discovery and validation cohorts. (**d**) BAAS accurately predicts (forced-choice classification) or strongly responds (one-sample t test) to high arousal experiences induced by stimuli across multiple modalities. Left panel: BAAS accurately predicts high arousing negative affect in studies 3 – 6 (total n = 210, prediction performance is shown as forced-choice classification accuracy (Cohen's d) or prediction-outcome correlation); Right upper panel: BAAS (marginally) significantly responds to high arousing positive affect in studies 7 – 16 (total n = 249); Right lower panel: BAAS accurately predicts high arousing negative and positive affect in study 17 (total n = 150, prediction performance is shown as forced-choice classification accuracy (Cohen's d)). See Table S1 for the details of each contrast. # Marginally significant, * P < 0.05, ** P < 0.01, *** P < 0.001. BAAS, Brain affective arousal signature. SCR, Skin conductance response.

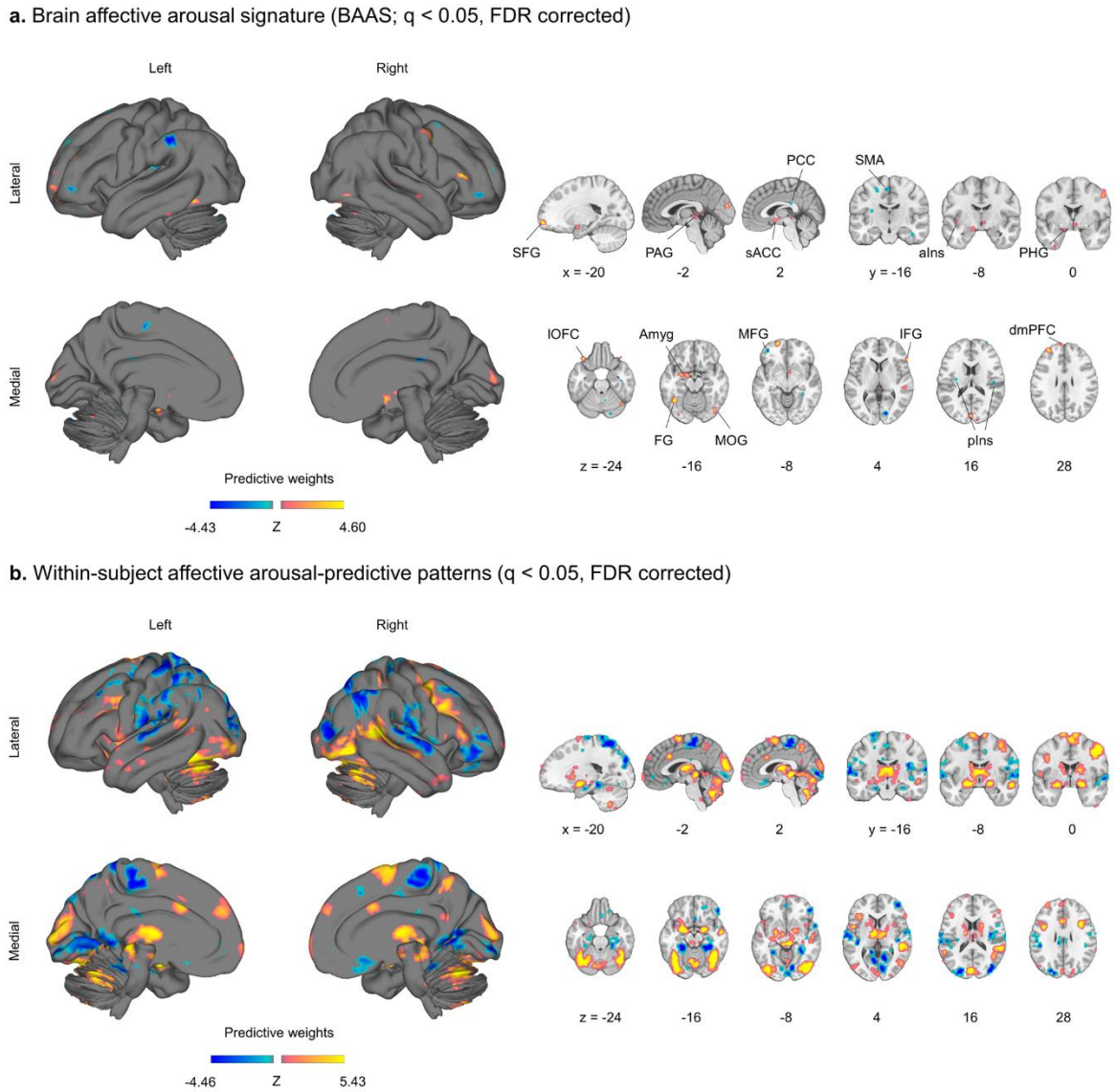

Fig. 3 Brain systems for affective arousal. (**a**) shows the thresholded BAAS. (**b**) summarizes multivariate patterns trained on individual subjects and depicts brain regions consistently predictive of subjective affective arousal across participants. All images are thresholded at q < 0.05, FDR corrected. Hot color indicates positive associations, whereas cold color indicates negative associations. BAAS, Brain affective arousal signature.

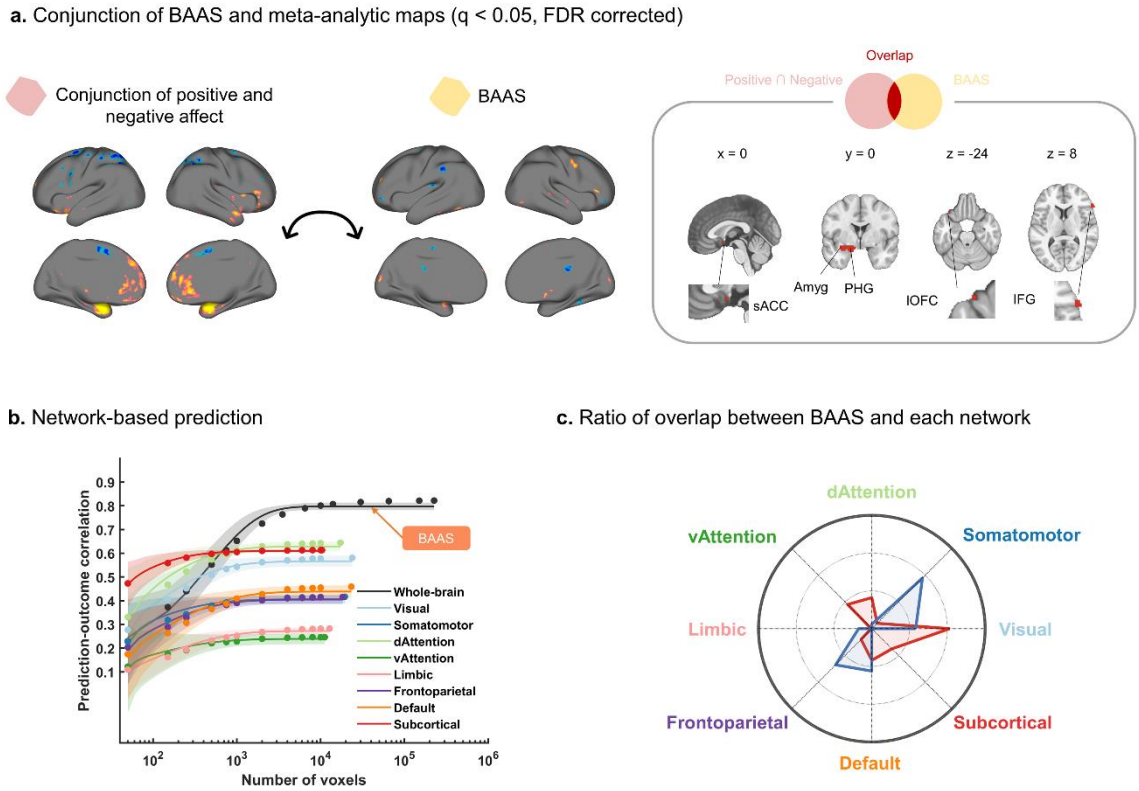

Fig. 4 The distributed neural representations of affective arousal exhibited neurobiological plausibility. (**a**) displays overlapping areas between thresholded BAAS and the conjunction of the meta-analytic maps of 'negative' and 'positive' affect from Neurosynth. (**b**) shows that the performance of the model was evaluated by using an increasing number of voxels/features (on the x-axis) to predict subjective affective arousal in different regions of interest, such as the whole brain (in black), subcortical regions (in red) or large-scale resting-state networks. The y-axis depicts the cross-validated correlation between predicted and actual outcomes. The colored dots demonstrate the average correlation coefficients, while the solid lines indicate the average parametric fit, and the shaded regions reflect the standard deviation. The model's performance is optimized by randomly sampling approx. 10,000 voxels across the entire brain. (**c**) shows the relative proportions of the voxels of thresholded BAAS within each large-scale functional network given the total number of voxels within each network. Red represents voxels with positive weight in the BAAS, while blue represents voxels with negative weight. BAAS, Brain affective arousal signature.

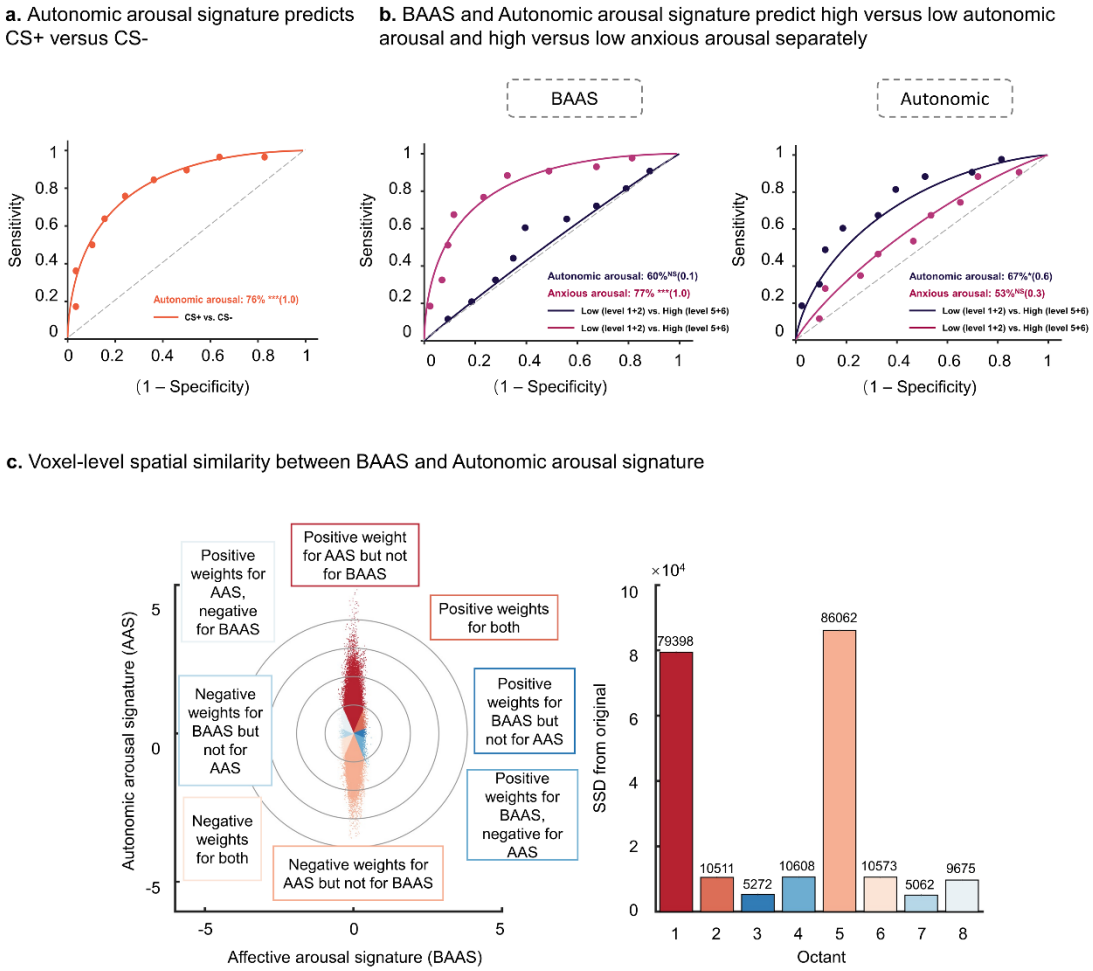

Fig. 5 Comparing neurofunctional decoders for affective arousal and autonomic arousal. (**a**) During a Pavlovian threat conditioning fMRI task (study 19), the developed autonomic arousal signature could predict CS+ (associated with high skin conductance level, SCL) versus CS- (associated with low SCL). (**b**) In study 20, BAAS more accurately predicts the anxious arousal experience during discrimination at high versus low intensity, while autonomic arousal more accurately predicts the autonomic arousal during discrimination at high versus low level. (**c**) Scatter plot displaying normalized voxel weights for affective arousal (BAAS, x-axis) and autonomic arousal (AAS, y-axis) signatures. Bars on the right side represent the sum of squared distances from the origin (0,0) for each Octant. Each Octant is assigned a different color, indicating voxels with shared positive or shared negative weights (Octants 2 and 6, respectively). Octant 1 represents selectively positive weights for the positive affect signature, Octant 3 represents selectively positive weights for the negative affect signature, Octant 5 represents selectively negative weights for the positive affect signature, Octant 7 represents selectively negative weights for the negative affect signature, and Octants 4 and 8 represent voxels with opposite weights for the two neural signatures. The numbers at the top of each bar indicate the number of voxels in each Octant. BAAS, Brain affective arousal signature. SCL, skin conductance level. CS, conditioned stimulus.

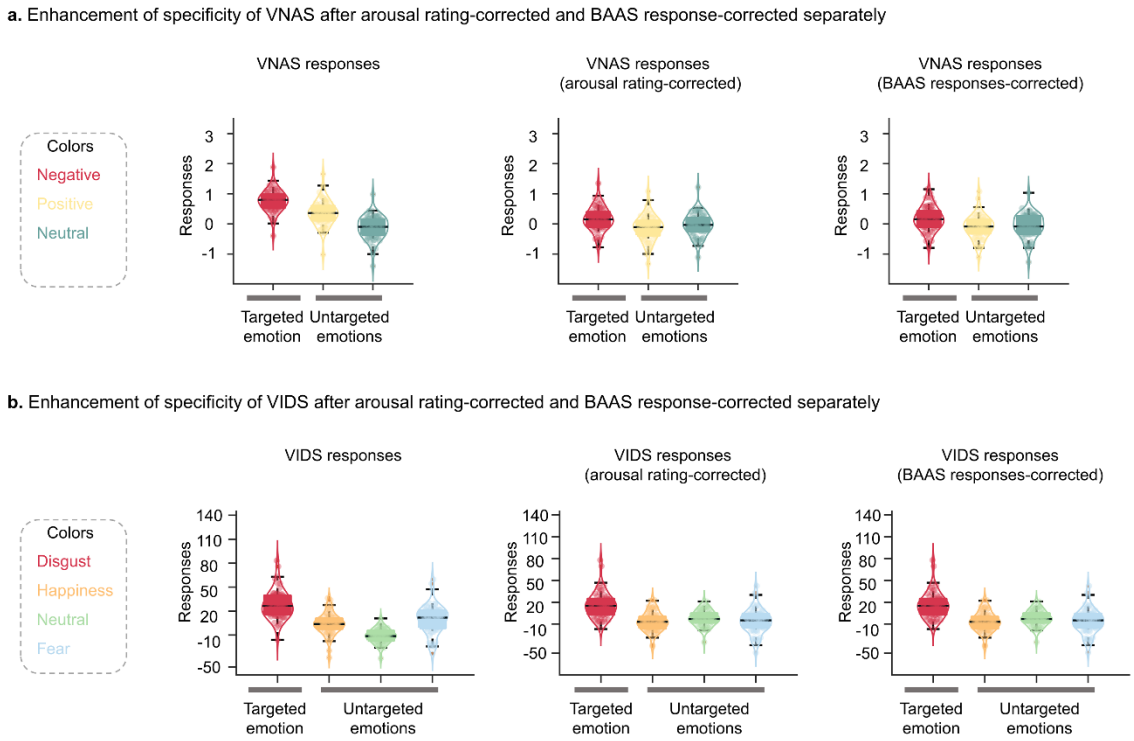

Fig. 6 The application of BAAS enhances the specificity of VANS and VIDS in study 1. (**a**), in the left panel, VNAS displayed higher responses to negative affect, while it also significantly responded to positive compared to neutral conditions; in the middle and right panels, after two correction methods (actual arousal ratings, BAAS response correction), VNAS showed similar responses to positive and neutral conditions. For details, see Supplementary Results. (**b**), in the left panel, VIDS showed higher responses to targeted emotion (i.e., disgust), while it significantly responded to happiness and fear compared to neutral emotions; in the middle and right panels, after arousal-rating-corrected or BAAS-responses corrected, VIDS still performed higher response to disgust, while it showed comparable responses to happiness, fear, and neutral emotions. VNAS, visually negative affect signatures, VIDS, visually induced disgust signature.